Silicone-recycled pyrolyzed fillers for enhanced thermal - and flame - resistant silicone elastomers

Raymond Hajj, Raphael Brunel, Rodolphe Sonnier, Claire Longuet, Francois Ganachaud

Silicone-recycled pyrolyzed fillers for enhanced thermal - and flame - resistant silicone elastomers

Raymond Hajj[a], Raphael Brunel[a], Rodolphe Sonnier[b], Claire Longuet[b], François Ganachaud[a,*]

[a] Université de Lyon - INSA Lyon, UMR CNRS 5223, IMP Ingénierie des Matériaux Polymères, F-69621, Villeurbanne, France
[b] Polymers Composites and Hybrids (PCH), IMT Mines Ales, Ales, France

A B S T R A C T

Two types of fillers were prepared by controlled pyrolysis of a commercial silicone elastomer. An aerobic process led to the formation of a silica powder while an anaerobic pyrolysis generated a silicon-carbon- oxide (SiOC) ceramic. Each filler was incorporated into a silicone gum and thus-prepared obtained formu- lations were further crosslinked with peroxide to prepare new silicone materials. Silica powder allowed controlling the mechanical properties of the materials whereas enhanced thermal stability was brought by the ceramic; mixing both fillers generated materials with joint properties (tensile strength of about 2 MPa, elongation at break of 300%, onset of degradation at 470 °C). The flame resistance behavior of these silicone materials was tested by cone calorimetry. Early formation of an insulating layer on the heat-exposed surface moderated the heat release (total heat release of 16.4 kJ/g $_{PDMS}$) and increased final residue (above 50%) compared to commercial silica-filled elastomers. This work opens new possibilities to transform silicone waste into useful inorganic fillers and produce new performant thermal-resistant silicone materials.

Keywords:
Silicone pyrolysis
Ceramic
Fillers
Fire resistance

1. Introduction

Silicone rubbers exhibit a unique combination of maintained elasticity at exceptionally low temperatures and high thermal and thermo-oxidative stabilities at high temperatures [1]. They are generally prepared by mixing silicone chains with reinforcing fillers and crosslinking the chains by different chemistries. The production of silicones has severely increased during the last decades [2] and the end-of-life of these complex composite materials remains an open question nowadays. Usually, most silicones end up as landfill waste [3] where they depolymerize within few days to few weeks [4–6]. They breakdown naturally into harmless byproducts such as oligomers containing silanol groups, silicates, CO_2 and H_2O [4–7].

Recycling silicones is not new per se. Early on, a team proposed to grind thermally-aged silicone rubbers to reintroduce these into the neat rubber formulation [8]. The addition of this powder at a loading of up to 60 phr caused acceptable losses in terms of tensile and tear properties in comparison to the genuine silicone rubber. Furthermore, the changes in hardness, hysteresis loss, tension set, and stress relaxation were found marginal.

Besides, more recently, several academic labs have proposed to recycle silicones by chemically degrading their network using metallic catalysts [9–11], fluoride catalysts [3,12,13], Lewis acids [11,14,15], strong acids [16], or strong bases [17]. The end-products are mostly silicone monomers that can then be used to produce again silicone elastomers and resins. For example, Enthaler and coworkers [10,11] have investigated the use of iron salts in the depolymerization of polysiloxanes to produce various types of silanes (e.g. dichlorodimethylsilane, diacetoxydimethylsilane, or dimethoxydimethylsilane). Typically, depolymerizing polydimethylsiloxane (PDMS) in a solution containing 7.5 mol% of FeF_3 with benzoyl chloride (190 °C, 5 h) resulted in 86% yield of dichlorodimethylsilane. Chang and coworkers [17] examined the base-catalyzed aminolysis of crosslinked PDMS to produce cyclic monomers (hexamethylcyclotrisiloxane (D_3), octamethylcyclotetrasiloxane (D_4), and decamethylcyclopentasiloxane (D_5)). The obliteration of silicone network occurred in a reactor containing potassium hydroxide as a basic catalyst, ethanol and diethylamine at room temperature to yield 80% of cyclic siloxane oligomers after 25 h.

Another conventional way of converting silicon-based polymers into useful materials consists in using them as precursors of ceramics, mainly for aerospace applications [18]. Several studies have long focused on the improvement of organic-to-inorganic conver-

* Corresponding author.
E-mail address: francois.ganachaud@insa-lyon.fr (F. Ganachaud).

sion of silicone rubbers by adding different catalytic systems into the network, so as to promote high residue yields and little volatile contents [19–22]. For instance, Liu and coworkers [20,21] used platinum-nitrogen- and platinum-thiol-based catalytic systems as ceramifying agents in silicone rubber. Thermogravimetric analyses showed that the final residue increased from around 1 up to 47% under nitrogen atmosphere and from 30 to 60 wt% under air in presence of the different systems at 900 °C. Delebecq and coworkers [19] investigated the synergistic role of platinum and silica as a way to increase the final residue of pyrolyzed silicones. The suggested degradation mechanism of polydimethylsiloxane (PDMS) in presence of these two components involves three steps: i) crosslinking reaction between PDMS chains adsorbed on silica via radicals generated by Pt at about 400 °C, ii) volatilization of PDMS mobile chain parts between 400 and 600 °C, and iii) ceramization of the remaining compelled chain fragments from 650 °C leading to the formation of a SiOC ceramic. Liquid silicone rubber (LSR) reinforced with vinylated-functionalized silica were shown to produce residues as high as 70 wt%. An original work by Shen and coworkers [23] explored the superhydrophobicity of SiOC powder obtained by burning silicone which showed some abrasion resistance and electro-conductive properties that opens some practical uses in e.g. electromagnetism shielding materials.

To the best of our knowledge, silica and other ceramics resulting from the degradation of silicone rubbers have never been reintroduced as fillers in silicone materials. In this work, we propose to pyrolyze a conventional commercial silicone elastomer in two different atmospheres and use these residues as fillers with the aim of bringing enhanced thermal properties to thus-prepared obtained new silicone rubbers.

2. Experimental

2.1. Materials

The pristine room-temperature-vulcanizing silicone (RTV) used in this study is an industrial two-part liquid component kit, containing a polymer base (part A) and a crosslinking curing agent (part B). The RTV crosslinks by hydrosilylation, and contains vinylated silica that allows a high residue content upon pyrolysis [19] (vide infra). A PDMS gum of weight average molar mass of about 500 kg.mol^{-1} was purchased from an industrial partner (see full description of gum A in ref. [24]). Luperox 101, 2,5-Bis(tert–butylperoxy)−2,5-dimethylhexane (DBPMH, technical grade, 90%) was purchased from Sigma-Aldrich. Commercial silica Aerosil A200 (hydrophilic fumed silica, specific surface 200 m^2/g) and Sipernat 22S (precipitated silica, 180 m^2/g) with silica contents of 99.8 and 97%, respectively, were kindly given by Evonik industries. All the products were used as received without any purification.

2.2. Preparation of fillers by RTV pyrolysis

In order to prepare high carbon content residues, the pristine crosslinked RTV silicone elastomer was cut into small parts of $2 \times 2 \times 1$ cm^3 placed in two interlocking steel tubes in order to limit air exposure. These tubes were then placed in an oven mounted in up to 850 °C, maintained around 15 min, then cooled down to room temperature (see the procedure described in [25]). The obtained black residue pieces (later named black ceramic powder or BCP) were then ground into powder. Furthermore, in order to prepare carbon-free residue, the same elastomer parts were pyrolyzed under air at 600 °C overnight. The obtained white residue was then ground into powder and pyrolyzed again overnight (still in air) to insure the total removal of the remaining carbon and finally obtain a white silica powder (abbreviated SP in the following).

2.3. Elastomers' preparation

The PDMS gum and a given filler were blended in a three-roll mill (EXAKT Advanced Technologies) for 20 min to obtain a homogenous paste and then, DBPMH was introduced at about 1% relatively to silicone fraction in the paste. The obtained mixture was vulcanized under thermal compression (8 MPa, 160 °C) for 30 min as in conventional high temperature vulcanization (HTV) procedure. Samples were then post-cured in an oven at 180 °C for 2 h. The addition of SP or BCP was adjusted to achieve a final filler content of 10, 30 and 50 wt%. For samples with mixed fillers, the PDMS was blended separately with 30% of either SP or BCP filler, and then the resulting silica-paste and ceramic-paste were mixed together in 25/75, 50/50 and 75/25 wt%. For comparative experiments, the PDMS gum was also blended with 30% of either Aerosil A200 or Sipernat 22S. Crosslinking procedure was the same for all samples.

2.4. Characterization methods

Fourier-transform infrared spectroscopy (FTIR) spectra were collected on a Bruker VERTEX 70 spectrometer with a diamond ATR probe at room temperature, and 32 scans were accumulated at a resolution of 4 cm^{-1}.

X-ray diffraction analyses (XRD) were performed at room temperature by using a BRUKER D8 Advance X-ray diffractometer. The X-ray beam radiation (Cu Kα, 1.542 Å) was operated at 40 kV and 40 mA. Data were obtained in the range of 2θ from 5 to 70°.

Solid-state nuclear magnetic resonance (NMR) analyses of aerobic and anaerobic residues were carried out on an AVANCE III 500WB spectrometer at 99.34 MHz (^{29}Si NMR) and 125.73 MHz (^{13}C NMR). Cross polarization magic angle spinning (CPMAS) and high-power proton decoupling (HPDEC) were performed on both nuclei. ^{29}Si CPMAS experiments were performed using a contact time of 5 ms, a recycling time of 5 s, a spinning rate of 10 kHz and 1000 scans. In the ^{13}C CPMAS experiments, the contact time was 3 ms, the recycling time 5 s, the spinning rate 10 kHz and the number of scans 5100. ^{29}Si HPDEC experiments were also performed using a recycling time of 120 s, a spinning rate of 10 kHz and 1700 scans. In ^{13}C HPDEC experiments, the recycling time was 60 s, the spinning rate 10 kHz and the number of scans 400.

The composition of aerobic and anaerobic residues was investigated on an X-ray photoelectron spectrometer (XPS, PHI Quantera SXM) with a monochromatic Al-Kα source. The detection angle was 45° and the analyzed area diameter was 200 µm. The detection limit was estimated at about 0.1 to 0.5 atomic% and the accuracy of the quantitative analysis at about 2 to 5% depending on the content.

The morphology of the filled silicones was observed using a scanning electron microscope (SEM, FEI Quanta 200). Micrographs were obtained under high vacuum at a voltage of 12.5 kV, with a working distance of 10 mm.

Hardness Shore A was measured on elastomers using a ZwickRoell (attached) durometer. Three measurements were applied on each of the samples (thickness $>$ 6 mm). Hardness values were recorded after 30 s of applying the device on the materials.

Thermogravimetric analyses (TGA) were performed under nitrogen (flow rate 90 mL.min^{-1}) using a Q500 apparatus from TA instruments. Samples ($5-8$ mg) were heated in platinum crucibles from 30 to 900 °C at a heating rate of 10 °C per minute.

2.5. Swelling experiments

Crosslink density and extractability of the prepared elastomers were evaluated through swelling experiments. About 0.3 g of an

elastomer sample (W_i) was immersed for 5 days (until equilibrium weight was considered to be reached) at room temperature in 5 mL of methylcyclohexane (MCH). The swelled sample was gently wiped to remove the liquid solvent present on the sample surface and weighted (W_s) then dried under vacuum overnight at 70 °C and weighted again (W_f). The extractable fraction (E) and the molar mass between crosslinks in the material (M_c^T) were calculated as described by Delebecq et al. [26] according to Flory–Rehner equation [27]. This molar mass considers both physical attachements, i.e. hydrogen bonds between silica surface and polymer backbone, and chemical nodes between PDMS chains. Swelling experiments were repeated under ammonia fumes to break the weak interactions between silica and PDMS chains [28, 29]. The molar mass between the chemical crosslinks (M_c ^{Ch}) was calculated as explained above. Each experiment was performed three times to ensure the reproducibility of the results.

2.6. Tensile testing

Tensile testing on elastomers were performed on an Instron 4469 apparatus according to ASTM D412. The dog bone-shaped samples had an effective length of 20 mm, a width of 4 mm, and a thickness of about 2 mm. The tensile measurements were performed using self-tightening roller tensile grips, long travel extensometer and pulling speed of 500 mm.min^{-1} until sample failure. Five samples were tested on each of the prepared elastomers. The plotted tensile curves were selected as the best performance obtained by each elastomer.

2.7. Cone calorimeter

Fire behavior of silicones was assessed on a FTT cone calorimeter according to ISO 5660. $100 \times 100 \times 4\,mm^3$ samples were burnt horizontally in air using an incident heat flux of 50 kW/m^2 in presence of a spark igniter. Each test was performed twice to ensure the reproducibility of the results. The heat release rate (HRR) was calculated according to the Huggett's equation [30] which states that 1 kg of consumed oxygen corresponds to 13.1 MJ of heat release. The balance support of the apparatus enabled following the evolution of the mass loss during the experiment. The residue yield originating from the PDMS part of the elastomer was calculated as the following

$$Residue = \frac{W_f - W_{fillers}}{W_{PDMS}} \times 100$$

where W_f is the weight of the sample fully burned, $W_{fillers}$ and W_{PDMS} are the weights of the fillers and PDMS in the elastomer before burning.

2.8. Thermal aging

Samples with 30% of different fillers were chosen to evaluate the aging properties of PDMS elastomers, together with pristine RTV. For this, five dog-bone shaped specimens were conditioned at 260 °C for 4 weeks consecutively. The samples were weighted before and after aging so as to measure the weight loss. Aging properties were assessed by tensile testing like described previously.

3. Results

3.1. Pyrolyzed powders

3.1.1. Preparation

The aerobic and anaerobic degradations of a commercial RTV silicone led to the formation of white and black powders, respectively. We have selected a specific grade that contains both vinylated silica and platinum, so that ceramization is greatly enhanced under inert atmosphere (see TGA spectrum in Figure S1). In aerobic degradation, we have pyrolyzed two times the materials, once using the original RTV material and one after grinding the residue, to remove all traces of carbon in the final powder (vide infra). The residues yield after aerobic and anaerobic degradation were 73 and 66%, respectively.

3.1.2. Characterization

FTIR spectra of both powders (Fig. 1a) were found close to the spectrum of a commercial silica (Aerosil A200). Two absorption bands were observed in the regions of 1000 – 1300 cm^{-1} and around 800 cm^{-1} assigned to the Si–O asymmetric stretching vibration [31,32]. The band corresponding to the asymmetric stretching vibration of Si–C is detected only for black ceramic, as expected. XRD analysis showed that the two prepared powders are amorphous with some metal oxide impurities originating from the preparation process (Fig. 1b). The main peak at 2θ around 20° entails all Si–O bonds of the materials. The shoulder prolonging to 40° in BCP indicates a large presence of SiOC units in the pyrolyzed ceramic.

XPS elemental analysis (Fig. 2) and solid NMR characterization (Figs. 3 and S2) were then confronted to provide finer information on the chemical structure of the pyrolyzed materials. ^{29}Si CPMAS and HPDEC routines were used here, the first non-quantitative but more sensitive technique to track the main peaks, and the second one to produce quantitative results (only the latter are commented below).

For the white powder, the surface of the ground sample presented an average composition of 28.3 ± 0.1 at% of silicon, 69.9 ± 0.3 at% of oxygen and some carbon traces around 1.8 ± 0.2 at% (at% = atomic percentage) (Fig. 2b). The Si2p peak shows a single component at 103.4 eV corresponding to silica [20,21]. The O1s peak decomposition shows the presence of two components where the majority of oxygen atoms (around 87%) at 532.7 eV corresponds to the Si-O bonds and the rest at 534.2 corresponds to adsorbed water. Despite the intensity of the noise, the weak C1s peak decomposition shows that carbon can be divided into three components: the first peak at 284.5 eV corresponding to Si–C or C–C bonds (around 70 at%), the second at 286.4 eV corresponding to C–O bonds (23 at%) and the third peak at 289.1 eV corresponding to O–C–O bonds (7 at%) [20]. This is a clear indication that low content of residual carbon is linked mostly to silicon atoms without affecting the silica structure (vide infra). These observations are in accordance with ^{29}Si HPDEC 10 KHz solid state NMR (Fig. 3b) that shows Q units of silicon into three sub-forms: 6 mol.% of Q_2 at –90 ppm, 28 mol.% of Q_3 at –99 ppm and 66 mol.% of Q_4 at –108 ppm.

XPS elemental analysis performed on the surface of the black powder determined the presence of 27.8 ± 0.2 at% of silicon, 57.2 ± 0.3 at% of oxygen and 15.0 ± 0.2 at% of carbon (Fig. 2c). The Si2p peak shows two types of silicon units which are 67 at% of Q units at 103.4 eV and 33% of D units at 102.1 eV [20,21]. The O1s peak shows two components which are 85% of Si-O bonds at 532.6 eV and 15% corresponding to adsorbed water at 534.2 eV. The C1s peak decomposition shows that the carbon signal can be divided into five components, among which main ones are at 283.4 eV (48% of total carbon) that corresponds to an undefined structure of carbon, and the second (40% of total carbon) at 284.6 eV corresponding to Si–C or C–C bonds. The other three minor forms of carbon at 286.4 eV (8%), 287.6 eV (1%) and 288.9 eV (3%) are due to different types of C–O bonds [20] (see Fig. 2c for details). ^{29}Si HPDEC solid state NMR showed that silicon atoms are present under their four forms: 21% corresponding to M units at 0 ppm ($SiOC_3$), 18% of D units at –29 ppm (SiO_2C_2), 26% of T units at –69 ppm (SiO_3C) and 35% of Q units at –100 ppm (SiO_4 where Q_3: 27.5% and Q_4: 7.5%) (Fig. 3d). The ^{13}C CPMAS spectrum did not

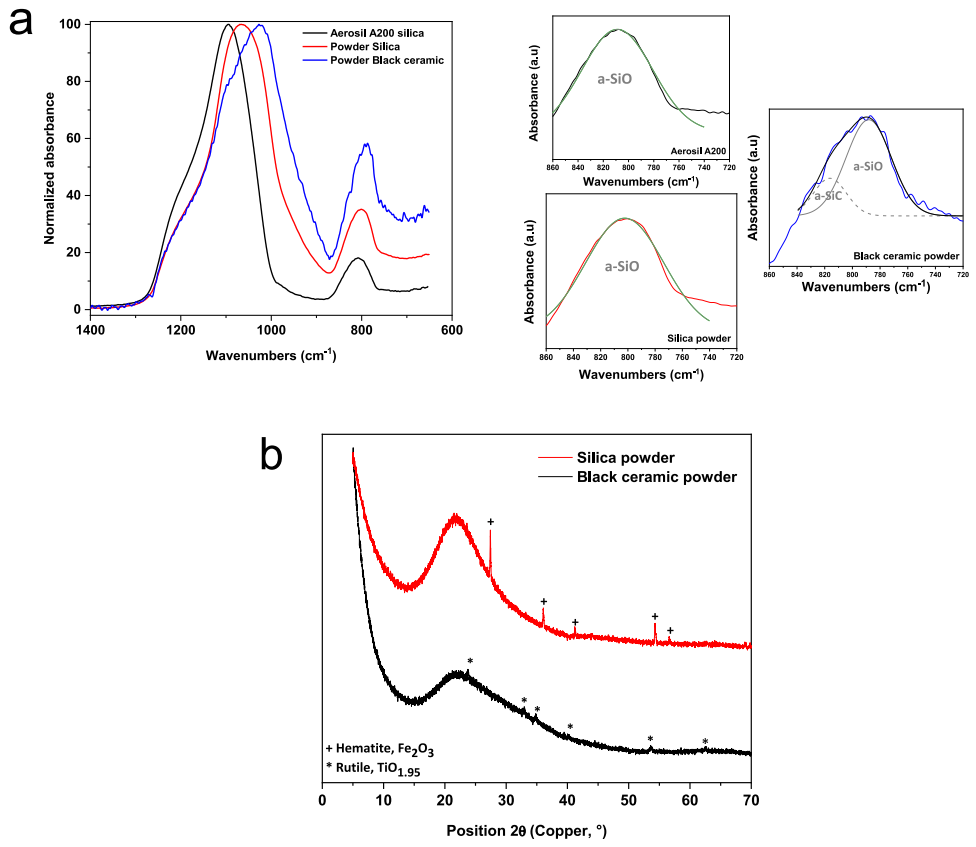

Fig. 1. (a) FTIR spectra of commercial silica Aerosil A200, silica and black ceramic powders and best gaussian fit(s) of main peak at about 800 cm^{-1}; (b) XRD analysis of silica powder and black ceramic powder.

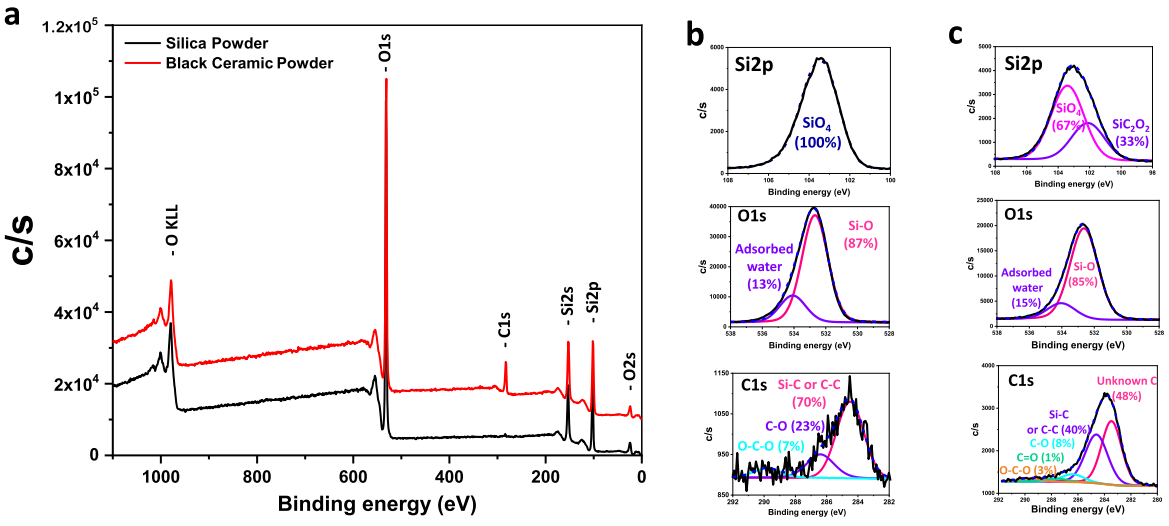

Fig. 2. (a) XPS wide scans for the silica powder and black ceramic powder; (b) Si2p, O1s and C1s XPS spectra for the silica powder; (c) Si2p, O1s and C 1 s XPS spectra for the black ceramic powder.

show peaks specific to a molecule or a group (Figure S2). Nevertheless, it was observed very broad bands in 2 areas of the spectrum, sp3 carbons between 10 and 50 ppm and sp2 carbons between 110 and 150 ppm, specific of aromatic compounds. The sp3 type of carbon could be mainly attributed to C–Si or C–C bonds observed in XPS while the sp2 type of carbon is attributed to aromatic compounds that could correspond to the unknown structure observed in XPS. Based on Kleebe and coworkers' works on the composition and the structure of RTV silicone residues obtained by pyrolysis under inert atmosphere [33,34], the appearance of aromatic compounds at 800 °C indicates the generation of a separate carbon phase from the ceramic one. Indeed, at this temperature, the pyrolysis induces a polymerization reaction of the methyl groups associated with removal of hydrogen atoms and a condensation reaction leading to the formation of aromatic compounds (as graphene for example).

In summary, XPS and ^{29}Si solid state NMR showed that the pyrolysis of an RTV elastomer under air proceeds via an oxidative crosslinking mechanism to essentially form large content of silica [21]. In the following parts of this study, this white powder

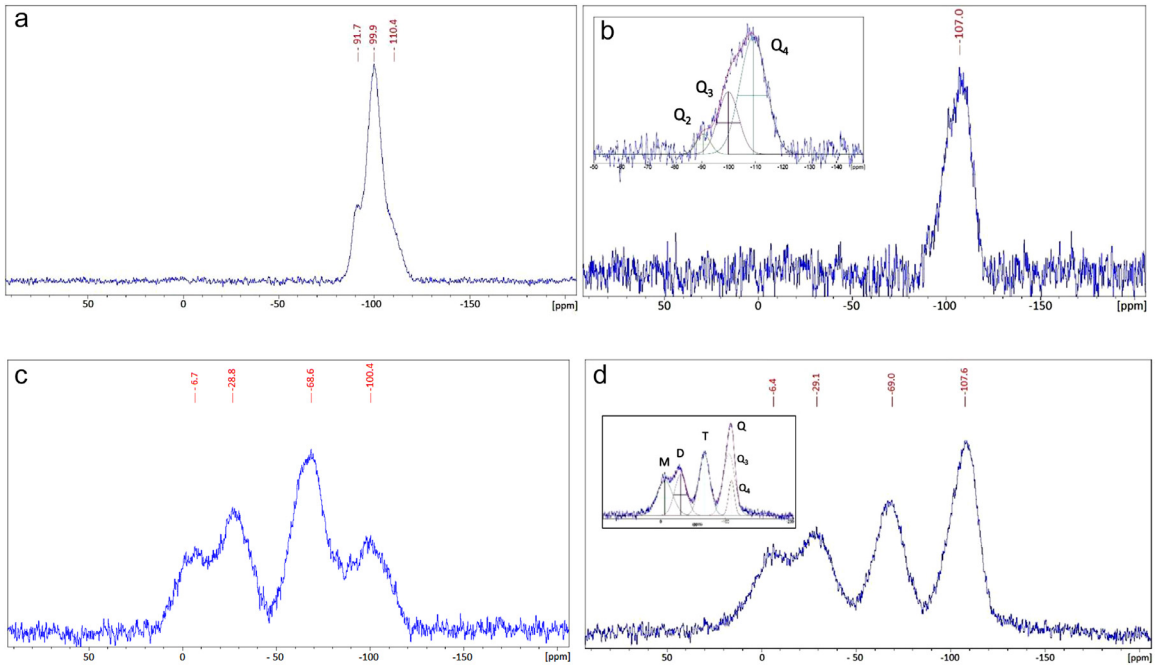

Fig. 3. Solid state NMR ^{29}Si 10 KHz spectra: (a) CPMAS of silica powder; (b) HPDEC of silica; inset: spectral decomposition. (c) CPMAS of black ceramic; (d) HPDEC of black ceramic; inset: spectral decomposition.

Table 1
All formulations tested in this study (as expressed in wt%).

	PDMS gum	Silica powder (SP)	Black ceramic Powder (BCP)	Commercial Silica	DBPMH
PDMS + 10% SP	89.20	9.91			0.89
PDMS + 30% SP	69.51	29.79			0.70
PDMS + 50% SP	49.75	49.75			0.50
PDMS + 10% BCP	89.20		9.91		0.89
PDMS + 30% BCP	69.51		29.79		0.70
PDMS + 50% BCP	49.75		49.75		0.50
PDMS + 30% mix (75% SP – 25% BCP)	69.51	22.34	7.45		0.70
PDMS + 30% mix (50% SP – 50% BCP)	69.51	14.90	14.90		0.70
PDMS + 30% mix (25% SP – 75% BCP)	69.51	7.45	22.34		0.70
PDMS + 30% Aerosil A200	69.51			29.79	0.70
PDMS + 30% Sipernat 22S	69.51			29.79	0.70

is referred to as “silica powder”, abbreviated as SP. The anaerobic degradation of same RTV led to carbon-carbon interchain crosslinking, due to the lack of oxygen, and produced a SiOC ceramic thanks to the synergic effect of silica and platinum. In addition, an independent aromatic structure of carbon a priori formed during the degradation process [19]. This “black ceramic powder” of rather complex structure is denominated BCP in the following.

3.2. New filled-elastomers

3.2.1. Preparation and microstructure

The two powders were introduced into a silicone gum via a three-rolls mill and crosslinked by peroxide activation to generate new HTV-type elastomer materials (see experimental part for details). All formulations tested in this study are summarized in Table 1.

Macroscopically speaking, homogeneous materials were produced with respective color induced by the filler (Figs. 4a and 4b). By SEM, both fillers were shown to have good compatibility with PDMS matrix (Figs. 4c and 4d). They exhibit random shapes with cutting edges, although XRD revealed that both fillers are amorphous, as anticipated from the moderate maximum temperature applied on pyrolysis (800 °C). As shown on SEM photos, the size distributions of fillers are qualitatively quite large, with particle sizes of silica powder estimated between 12 and 15 µm, and homogenous distribution within the matrix. On the other hand, we observed mainly two size categories for BCP elastomer, the first one is less than 5 µm while the second is around 20 µm. In fact, during the preparation of the pastes, the fillers are crushed between the two rolls so that the maximum size of the fillers is about 20 µm.

3.2.2. Crosslink density

Swelling experiments were carried out in normal atmosphere or under ammonia fumes, the latter which breaks interactions between the silanol groups on the filler and the silicone chains. All results are summarized in Table 2. For SP samples, M_c^T (M_c total, obtained in normal atmosphere) decreases from around 17,500 to 6400 g/mol when silica powder fraction increased from 10 to 50%, respectively. Chemical M_c^{Ch} (under ammonia fumes) shows the same trend with a systematic difference of 2500 g/mol compared to M_c^T for all samples. Interactions between silica and PDMS chains do not affect much the M_c^T, as expected from a filler with a relatively low specific surface (according to the average size of the filler particles). On the other hand, the results show that the crosslink density increases with silica content, which was an unexpected result. The extractable amounts were found constant, around 4% at all silica contents, indicating mostly full crosslink-

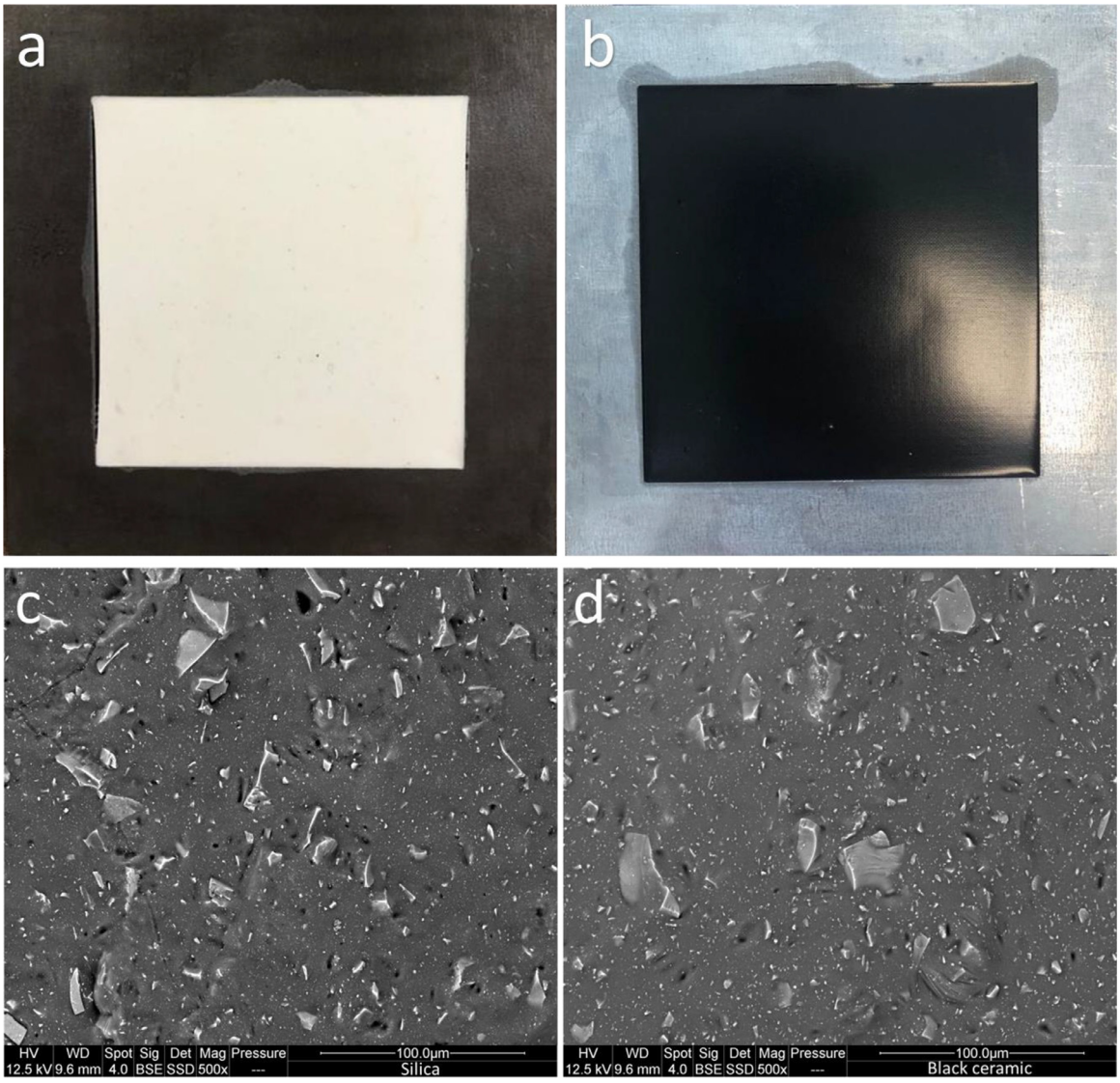

Fig. 4. (a, b) Photographs of the elastomers containing 30 wt% of silica powder (a) and black ceramic powder (b) after peroxide crosslinking; (c, d) Corresponding SEM micrographs of elastomers filled by silica powder (c) and black ceramic powder (d). Note that the black spots observed on the SEM micrographs are ascribed to an uncomplete metallization (see also Figure S3).

Table 2
Data collected from swelling tests in methylcyclohexane (MCH) under air atmosphere and under ammonia fumes (swelling content and extractives in %) as well as crosslinking density evaluation (total molar mass between two nodes M_c^T and molar mass between two chemical crosslinks M_c^{Ch}).

	MCH			MCH under ammonia fumes		
	Swelling (%)	M_c^T (kg/mol)	Extractives (%)	Swelling (%)	M_c^{Ch} (kg/mol)	Extractives (%)
PDMS + 10% SP	334 ± 3	17.5 ± 0.5	4.2 ± 0.4	361 ± 2	20.0 ± 0.07	3.3 ± 0.5
PDMS + 30% SP	203 ± 1	10.6 ± 0.2	3.8 ± 0.8	229 ± 1	12.8 ± 0.04	1.9 ± 0.3
PDMS + 50% SP	112 ± 0	6.4 ± 0.2	4.0 ± 0.8	138 ± 2	9.0 ± 0.20	1.2 ± 0.2
PDMS + 10% BCP	400 ± 5	24.8 ± 0.6	3.9 ± 0.2	407 ± 2	25.2 ± 0.20	2.9 ± 0.7
PDMS + 30% BCP	444 ± 2	54.0 ± 0.5	6.5 ± 0.3	508 ± 4	65.9 ± 2.4	3.8 ± 0.9
PDMS + 50% BCP	340 ± 10	220 ± 12	48.5 ± 0.4	374 ± 6	300 ± 6	51.9 ± 0.2
PDMS + 30% mix (75% SP – 25% BCP)	220 ± 2	12.1 ± 0.05	3.0 ± 0.7	242 ± 3	14.4 ± 0.5	2.2 ± 0.4
PDMS + 30% mix (50% SP – 50% BCP)	230 ± 1	13.2 ± 0.2	2.6 ± 0.3	253 ± 2	15.7 ± 0.4	2.0 ± 0.8
PDMS + 30% mix (25% SP – 75% BCP)	254 ± 7	15.4 ± 0.3	2.2 ± 0.4	282 ± 1	19.1 ± 0.2	1.1 ± 0.2

ing of the elastomer. Note that we checked that a formulation not containing peroxide precursor does not crosslink in the same conditions since we obtained after tentative vulcanization the same viscoelastic paste as originally prepared (not shown).

Materials containing a PDMS matrix filled with black ceramic were difficult to crosslink. Molar masses between two chemical crosslinks in PDMS/BCP elastomers increase exponentially from around 25,000 to around 300,000 g/mol at increasing BCP content (from 10 to 50%) whereas the extractable amounts rises from 4% to around 49%. This is a clear indication that black ceramic impeded PDMS crosslinking. The black ceramic is composed in part of a carbon phase containing aromatic carbon rings that are known

Table 3
Mechanical properties data: Hardness Shore A and tensile testing of the different elastomers.

	Hardness Shore A	Stress at break (MPa)	Elongation at break (%)
PDMS + 10% SP	19 ± 1	0.59 ± 0.04	240 ± 20
PDMS + 30% SP	31 ± 1	1.62 ± 0.11	310 ± 30
PDMS + 50% SP	55 ± 0	2.82 ± 0.10	240 ± 10
PDMS + 10% BCP	15 ± 1	0.69 ± 0.11	450 ± 90
PDMS + 30% BCP	17 ± 1	1.36 ± 0.05	1050 ± 150
PDMS + 30% mix (75% SP – 25% BCP)	30 ± 1	1.68 ± 0.08	330 ± 20
PDMS + 30% mix (50% SP – 50% BCP)	27 ± 1	1.57 ± 0.04	350 ± 20
PDMS + 30% mix (25% SP – 75% BCP)	26 ± 1	1.51 ± 0.13	360 ± 30

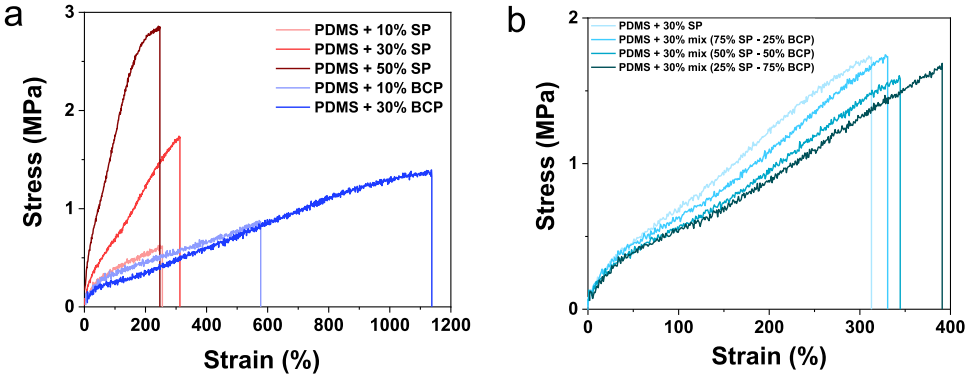

Fig. 5. Stress – strain curves of PDMS/SP or BCP elastomers (a) and PDMS/mixed fillers elastomers (b).

to kill radicals [35], which may thus explain such difficult curing step. Typically, the sample of PDMS filled by 50% was not enough crosslinked to be further considered as a material. Note finally that at 10% of black ceramic, physical interactions seem to be negligible contrary to what was observed for SP-filled materials.

Mixing both fillers in PDMS matrix led to a behavior similar to elastomers filled with silica. The molar mass between two chemical crosslinks is around 13,000 g/mol for PDMS filled with 30% silica only and rises linearly from around 14,000 to around 19,000 g/mol relatively to black ceramic fraction. M_c^T versus M_c^{Ch} is only about 2000 g/mol difference, as for silica-filled samples. Finally, extractables amounts are less than 4% in these mixed formulations. Hence, it shows that even a small amount of silica in these elastomers is enough to allows a full crosslinking of the samples even in presence of black ceramic.

3.2.3. Mechanical properties

A summary of the different techniques and data gathered from this part is given in Table 3.

First, materials' hardness was measured for all samples. Those containing SP showed fair hardness value improved by increasing SP content (Table 3) to reach a value of 55 Shore A at 50% SP.

Tensile properties also clearly rised with SP contents (Fig. 5). Stress at break increased from 0.59 ± 0.04 to 1.62 ± 0.11 and 2.82 ± 0.10 MPa for 10, 30 and 50% of SP, respectively. Strain at break was about 250% for all three samples. This shows that silica hardens the PDMS matrix thus leading to high mechanical properties [1].

For elastomers filled with black ceramic, stress at break increased from 0.69 ± 0.11 to 1.36 ± 0.05 MPa for materials filled with 10 and 30% of BCP, but in the meantime, strain at break increased from 450 ± 90 to 1050 ± 150%, respectively. At 50 wt% of ceramic filler, the material was so soft that tensile properties could not be assessed. Besides, hardness values were maintained around 17 Shore A (Table 3). As discussed previously, black ceramic partly inhibits PDMS vulcanization that in fact limits the final mechanical properties of the elastomers (particularly tensile strength).

Tensile properties of materials prepared with mixed fillers were also studied (Fig. 5b, Table 3). Stress at break plateaued around 1.60 ± 0.10 MPa, whereas strain at break increased slightly while substituting a fraction of silica powder by black ceramic powder. These results are in accordance with the swelling observations. The presence of a small content of silica powder in the initial formulation was enough to reach a full vulcanization of the material and thus to bring sufficient toughness to the materials. As the black ceramic fraction increased, the crosslinking density declined, which can explain the slight rise of strain at break. Additionally, shore A hardness slightly declined because black ceramic softened the material (Table 3).

Note that samples prepared with commercial silicas logically exhibited better tensile properties, thanks to their larger specific surface and thus higher reinforcing behavior [36] (Figure S4).

3.2.4. Thermogravimetric analyses

The different elastomers were analyzed by TGA under nitrogen atmosphere (Fig. 6 and Table 4). Pristine (uncrosslinked) PDMS gum presents mainly one degradation step (according to the derivative curve – Fig. 6b). The onset temperature of PDMS was observed at 400 °C and residual weight was negligible. Both incorporation of SP into silicone gum and crosslinking reaction increased significantly the thermal stability of the final material. Onset temperature rose to 410, 440 and 470 °C in accordance with incorporated silica rate into the elastomers, respectively 10, 30 and 50 wt% of SP. In a similar manner, thermal stability was much improved in presence of BCP. It rose to 460, 490 and 520 °C, respectively, while increasing the amount of black ceramic from 10 to 30 and 50 wt%. A significant jump of + 120 °C is thus observed between pristine PDMS and material at 50 wt% of BCP.

Looking at the derivatives of TG curves, one sees that the degradation process changed from silica- to black ceramic-based materials. A first degradation step occurs around 560 °C while a second one takes place around 660 °C. According to the intensities of the peaks in the derivative curves, the first degradation step of PDMS/BCP elastomers is less pronounced than in the case of PDMS/SP, whereas second peaks are higher to finally lead to almost

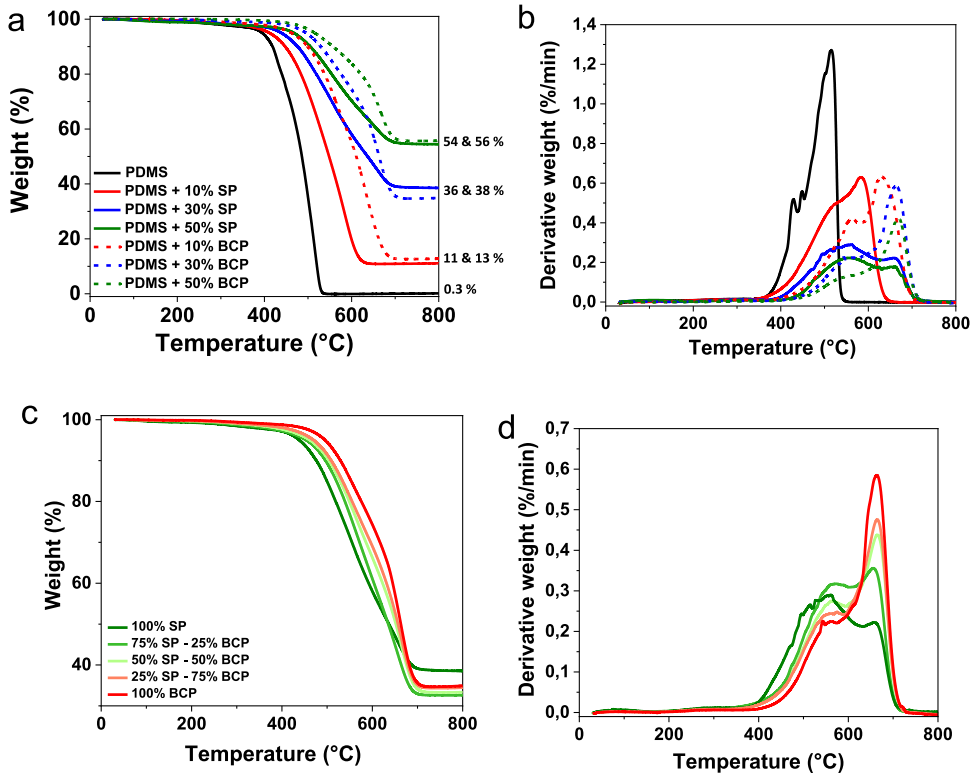

Fig. 6. Influence of fillers ratio on the thermal stability of the different elastomers prepared in this study: (a) TG curves of monofiller samples; (b) DTG curves of monofiller samples; (c) TG curves of mix-filled samples; (d) DTG curves of mix-filled samples.

Table 4
Main data measured by TGA.

	T_{onset} (°C)	T_{10} (°C)	$T_{max,1}$ (°C)	$T_{max,2}$ (°C)	Peak dTG_1 (%/min)	Peak dTG_2 (%/min)	Residue at 800 °C (%)
PDMS	400	420	510	N/A*	1.3	N/A*	0.3
PDMS + 10% SP	410	450	580	N/A*	0.6	N/A*	11
PDMS + 30% SP	440	480	560	660	0.3	0.2	38
PDMS + 50% SP	470	510	560	660	0.2	0.2	54
PDMS + 10% BCP	460	500	560	630	0.4	0.6	13
PDMS + 30% BCP	490	530	550	660	0.2	0.6	36
PDMS + 50% BCP	520	560	ND*	670	ND*	0.4	56
PDMS + 30% mix (75% SP – 25% BCP)	450	495	560	660	0.3	0.3	33
PDMS + 30% mix (50% SP – 50% BCP)	460	505	570	660	0.3	0.4	34
PDMS + 30% mix (25% SP – 75% BCP)	470	510	570	660	0.2	0.5	35
PDMS + 30% Aerosil A200	460	490	570	N/A*	0.7	N/A*	32
PDMS + 30% Sipernat 22S	430	480	560	N/A*	0.6	N/A*	29

*ND = not determined; N/A = not available.

similar residues. Therefore, black ceramic stabilized thermally the silicone elastomers and shifted the maximal degradation to higher temperatures. A slight increase in residual weight of about 4 to 8% was noticed compared to the expected one when considering the introduced filler content (Fig. 6a), especially with high amount of fillers, a priori thanks to the presence of residual platinum from RTV [19], without any influence of the composition of the fillers (Table 4).

The effect of mixing black ceramic and silica powders on the thermal stability of PDMS was carefully studied (Fig. 6c). Elastomers with mixed fillers showed a two-step degradation process occurring at the same temperatures as mentioned previously for mono-filled samples. It was clearly observed that increasing the content of black ceramic in the mix would decrease the first degradation step intensity and increase the second one (see derivative curves in Fig. 6d, Table 4). Moreover, increasing the amount of black ceramic in the mixes would increase the onset temperature of the material. In the following, the sample containing 30% of mixed fillers (25% silica and 75% black ceramic powders) was particularly selected for further tests as it shows both fair mechanical properties and high thermal stability.

The effect of other types of commercial filler on thermal properties of PDMS was also studied here for comparison (Figure S5 and Table 4). Onset temperatures of elastomers shifted only by + 30 to + 60 °C when filled by commercial silicas compared to PDMS, while in the case of recycled silica and black ceramic samples, it shifted by +40 to + 90 °C for the same amount of fillers (Table 4). Moreover, a single degradation step was observed around 560 °C for the elastomers filled with commercial silicas, alike PDMS case, which occurs at the same temperature as the first degradation of elastomers containing pyrolyzed fillers (Figure S5). All those results show a clear improvement of the thermal stability of elastomers filled with recycled powders in comparison to commercial silica.

Table 5
Tensile data before and after aging of samples containing 30% of fillers and pristine RTV.

		Before thermal aging		After thermal aging		
		Stress at break (MPa)	Strain at break (%)	Stress at break (MPa)	Strain at break (%)	Weight loss (%)
Filler type	SP	1.62 ± 0.11	310 ± 30	0.81 ± 0.04	70 ± 7	9.5 ± 0.4
	BCP	1.36 ± 0.05	1050 ± 150	0.70 ± 0.04	40 ± 2	7.6 ± 0.0
	Mix (25% SP – 75% BCP)	1.51 ± 0.13	360 ± 30	0.73 ± 0.02	40 ± 1	7.9 ± 0.1
	Aerosil A200	8.67 ± 0.50	350 ± 20	NM*	NM*	17.1 ± 0.0
	Sipernat 22S	8.07 ± 0.54	330 ± 30	1.96 ± 0.07	20 ± 2	7.5 ± 0.3
Pristine RTV	6.26 ± 0.34	600 ± 20	NM*	NM*	14.9 ± 0.1	

*NM = Non-measurable.

Table 6
Main data from cone calorimeter.

	TTI (s)	pHRR (kW/m²)	THR (kJ/g)	THR (kJ/gPDMS)	Residue (%)
PDMS + 10% SP	59 ± 2	201 ± 11	17.1	19.0	45
PDMS + 30% SP	46 ± 8	198 ± 13	11.4	16.3	46
PDMS + 50% SP	44 ± 5	167 ± 19	7.7	15.3	59
PDMS + 10% BCP	27 ± 4	198 ± 21	15.8	17.6	39
PDMS + 30% BCP	39 ± 3	186 ± 11	11.6	16.5	50
PDMS + 30% mix (25% SP −75% BCP)	45 ± 1	169 ± 18	11.5	16.4	51
PDMS + 30% Aerosil A200	73 ± 0	219 ± 4	13.4	19.2	41
PDMS + 30% Sipernat 22S	57 ± 3	202 ± 12	12.8	18.2	37
Pristine RTV	73 ± 2	142 ± 4	9.0	12.7[a]	71[a]

[a] on the basis of 29 wt% of silica in the RTV.

3.2.5. Thermal aging resistance

Dog-bone shaped specimens of elastomers filled by 30% of several fillers were conditioned at 260 °C for 4 weeks consecutively. After that, samples were weighted and evaluated by tensile testing (Table 5, Figure S6). All samples clearly lost most of their properties in such harsh conditions, but differences could still be stressed out. Samples containing pyrolyzed fillers showed the best aging resistance among the tested fillers. Weight losses were between 7.5 and 9.5% after 1 month at 260 °C. Samples filled by 30% of SP showed the best mechanical properties after aging. The tensile properties of PDMS/SP went from strain at break of 310% and a corresponding stress of 1.6 MPa to 70% and 0.8 MPa respectively after aging (Table 5 and Figure S6). Moreover, samples of PDMS/BCP and PDMS/mixed fillers had higher losses of properties to reach 40% and 0.7 MPa of strain and stress at break after aging.

For comparison, the Aerosil elastomer did not withstand thermal aging; it lost around 17 wt% during the aging process and became breakable during the preparation for tensile testing. The Sipernat elastomer had a better behavior with weight loss close to the other fillers, but sharp decrease of strain at break (compare Figure S4 and Figure S6). Pristine RTV lost around 15% in weight after 4 weeks of aging and the specimens were very brittle and breakable immediately when preparing tensile test. In summary, the pyrolyzed fillers brought enhanced resistance to long term thermal aging compared to other conventional materials.

3.2.6. Fire behavior

The influence of silica and black ceramic powders on the flame retardancy of corresponding elastomers was tested by cone calorimeter. In addition, the material prepared with mixed fillers (25% SP – 75% BCP) was carefully chosen among this series of samples according to its best mechanical and thermal properties (Fig. 7 and Table 6). For comparison, the materials prepared from the two commercial silica fillers have also been tested, as well as the pristine RTV (see Figure S7 and Table 6).

Elastomers filled with Aerosil A200 and Sipernat 22S ignited after 73 ± 0 s and 57 ± 3 s of exposure to heat flux respectively. The pHRR was reached 40 s after ignition and HRR maintained at around 200–220 kW/m^2 for around 150 s. After this plateau, HRR decreased, surely thanks to an insulating layer produced on the top of the sample (see white solid platelets in Figure S8) until the flame-out. THR was calculated around 19 kJ/g_{PDMS} and residue yield around 40% (see experimental part for calculation). This residue yield calculation is specific to silicone materials since silicon-based volatiles oxidize during the test, resulting in an amorphous silica-ash deposition on the surface of the samples [37]. The same general behavior was observed with pristine RTV, which ignited after 73 ± 2 s before reaching a plateau at HRR around 140 kW/m^2 for around 140 s, except that residue was much larger (around 70%) and THR smaller (12 kJ/g_{PDMS}).

Samples with pyrolyzed fillers (silica, black ceramic or a mix of both) exhibited a behavior significantly different (Fig. 8 and Table 5). BCP-filled elastomers ignited relatively faster with a time-to-ignition around 40 – 45 s for 30% of fillers. Few seconds after TTI, the pHRR reached 170–200 kW/m² depending on the nature and the content of fillers, i.e. slightly lower than the values obtained for elastomers filled with commercial silica. But the pHRR decreased sharply and no HRR plateau was observed. This evidences that the insulating layer was forming faster and then protected more efficiently the underlying material than commercial silica. The THR was found around 16.5 kJ/g_{PDMS} independently of the fillers' composition. Moreover, the residue yield for filler-recycled elastomers ranged between 46 and 51% relatively to silicone gum weight. This value is higher than for elastomers filled with commercial silicas.

4. Discussion

In this work, we have proposed to pyrolyze a commercial silicone RTV into two different powders to be tested as fillers in new high temperature vulcanization (HTV) formulations. Depending on the surrounding atmosphere, air or nitrogen respectively, either silica or black ceramic powders were prepared in quantitative yield. They were fully characterized by different techniques (ATR-FTIR, XPS and NMR) to confirm the overall microstructure of the residues. In the anaerobic process, a significant content of aromatic carbons was generated in addition to the SiOC ceramic, a result that was previously described [19,25]. Whereas, the aerobic process led in two steps to almost full silica material.

After grinding, both fillers were introduced in a high molar mass silicone gum to generate homogeneous materials (accord-

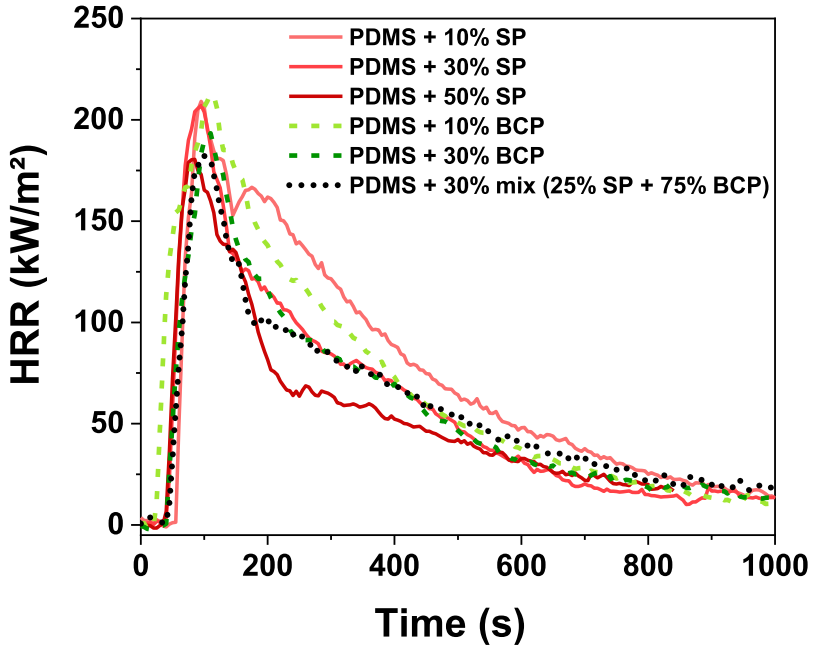

Fig. 7. Influence of pyrolyzed fillers' type and content on HRR curves of PDMS elastomers (heat flux 50 kW/m^2).

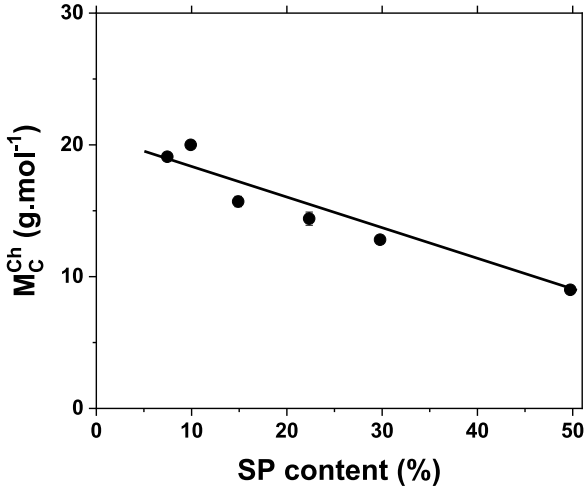

Fig. 8. Influence of the silica powder content on the M_C^{Ch} for SP and mixed fillers elastomers.

ing to SEM photos) after peroxide crosslinking. The obtained elastomers were then tested by conventional techniques (swelling, tensile tests). Two opposite behaviors were obtained in terms of crosslinking reaction. Increasing the silica powder content resulted in more crosslinked materials, and thus stronger materials both in hardness in tensile strength. Contrarily, black ceramic was shown to inhibit partially the crosslinking reaction, limiting its use at high content. When mixing both of the fillers, crosslinking proceeded smoothly and mechanical properties were close to silica-filled materials.

We suspect that silica could participate to the crosslinking reaction in one way or another, generating strong materials even without reinforcement (large particle flakes mean low specific surface). Removing the peroxide initiator from the formulation did not lead to crosslinking, so silica is not able to promote crosslinking by itself. Two hypotheses can then be brought: 1. Crosslinking of the chains with the surface group of silica naturally reinforcing the materials; 2.'boosting' effect of silica powder towards the generation of radicals and thus enhanced crosslinking reaction. We have shown that inhibition induced by the black ceramic could be suppressed when adding even a small amount of silica. Also, the chemical crosslinking density of all samples containing SP is in direct correlation with the silica content (Fig. 8). Finally, the extractive content decreased with silica powder content in both simple filler or mixed filler samples and these were found much lower than generally observed in peroxide-crosslinked materials. All this information pleads for an accelerating effect of radical generation when introducing silica powder. The chemistry behind that phenomenon still remains to be understood.

Mechanically speaking, some correlations can be established, independent of the content and nature of pyrolyzed fillers. We observed that the strain at break rises rather linearly when the molar mass between two chemical crosslinks increases, showing that the network density correlates well with the plasticity of the materials (Fig. 9a). Moreover, the tensile strength rises linearly with hardness shore A, both parameters depending directly on the strength of the elastomers (Fig. 9b). We also showed that the content of extractive materials was slightly depressed in mix-filled elastomers compared to SP and BCP filled ones, showing a synergy of properties between the two fillers in the mix material.

Looking at thermal properties, TGA showed that the black ceramic significantly shifted the onset of degradation of the materials of more than 100 °C, whereas the white silica powder increased the residue of only 50 °C. In the mix filled systems, a direct linear correlation is observed between main transitions and composition (Fig. 10). Note that filler-recycled elastomers' TGA residues were only slightly increased, showing that platinum traces from RTV precursor hardly promoted ceramization of the new recycled materials. To compare these results with literature data, we have reported in Table 4 the temperature of degradation of 10% of the sample (T_{10}). Liu and coworkers [21,22] improved the T_{10} values of silicones by 40 °C by adding Pt (Karstedt catalyst) and nitrogenous silane systems while Liu and coworkers [20] improved it by 20 °C by adding 50 ppm of Pt (Karstedt catalyst) and 0.2 phr of (3-mercaptopropyl)triethoxysilane. Here, new pyrolyzed fillers clearly improved the thermal stability of corresponding elastomers.

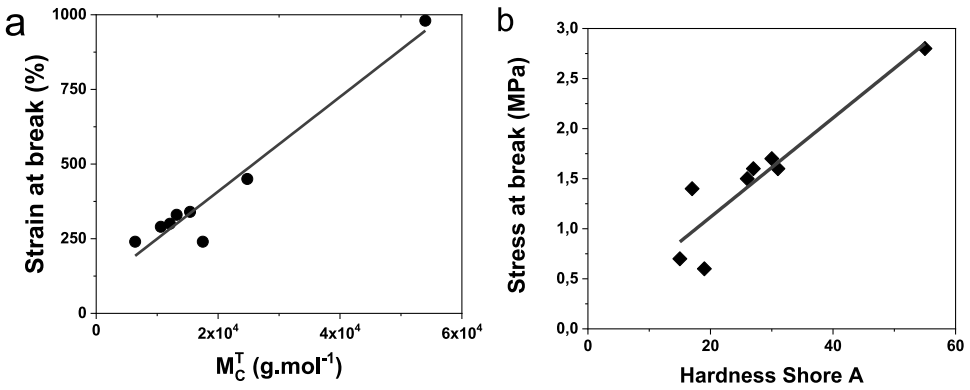

Fig. 9. Influence of the network crosslinking on the strain at break versus M_c^T (a) and the hardness shore A versus stress at break (b) for all filler-recycled elastomers prepared here.

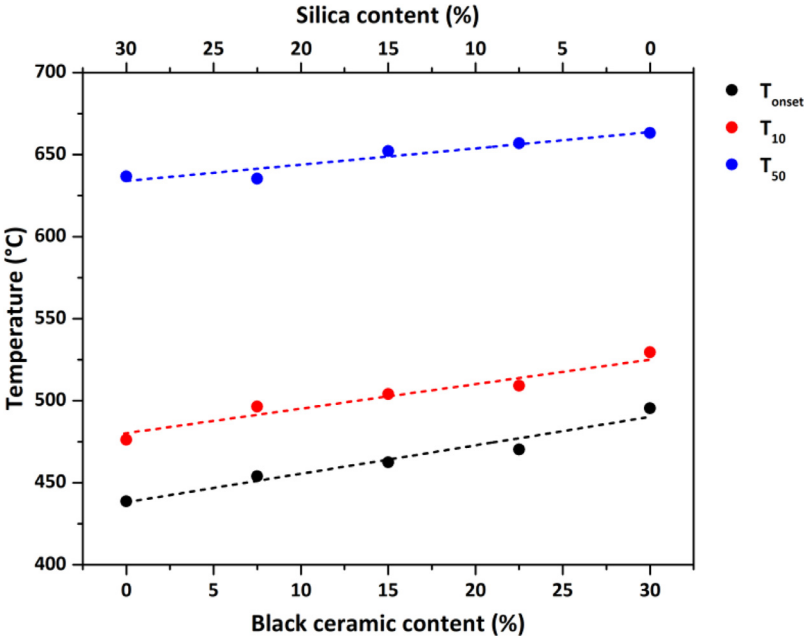

Fig. 10. Influence of silica powder and black ceramic powder content on onset temperature and temperature at 10% and 50% of degradation of PDMS.

During thermal aging, PDMS chains degrade to shorter oligomers in one hand, whereas on the other hand, radical coupling increases the crosslink density [21]. The result of these is an enhanced brittleness. For the two pyrolyzed fillers, the mechanical properties were greatly affected, particularly in terms of tensile strength, but still materials could be tested. Neither pristine RTV nor aerosil-filled sample sustained such long aging cycle, since their mechanical properties could not be tested.

Finally, flame retardancy was studied by cone calorimetry. Even if the TTI is reached more rapidly for filler-recycled elastomers than conventional ones, the rapid generation of a thick barrier layer promoted slow burning, low heat release and a larger final residue yield. Such behavior is expected from the fact that introduced fillers are per se resistant to pyrolysis.

5. Conclusions

In this work, a new single-step solution of reusing RTV silicone waste was studied. Two types of residues were prepared and used as fillers in a silicone matrix. The silica powder brought some fair mechanical properties to the elastomers while the black ceramic incredibly improved TGA thermal properties. Mixing both fillers in a single material brought sufficient mechanical properties while avoiding crosslinking inhibition observed for black ceramic formulations. The elastomer containing 30% of fillers (75% of black ceramic and 25% of silica) showed the best compromise in terms of mechanical and thermal properties. Moreover, these fillers improved the thermal resistance of elastomers compared to those containing commercial silicas. Finally, the filler-recycled elastomers prepared in this work showed better flame retardancy behavior than pristine RTV or elastomers filled with commercial silicas. It forms an insulating layer on the heat-exposed area earlier than commercial fillers which brings more protection to the matrix and results in less heat release. Overall, this work adds a new solution for one of the actual environmental issues by reducing silicone waste and reducing the use of raw materials for preparing fillers for silicone materials.

Declaration of Competing Interest

The authors declare that they have no known competing financial interests or personal relationships that could have appeared to influence the work reported in this paper.

CRediT authorship contribution statement

Raymond Hajj: Investigation, Formal analysis, Writing – original draft, Project administration. **Raphael Brunel:** Investigation. **Rodolphe Sonnier:** Investigation, Writing – review & editing. **Claire Longuet:** Writing – review & editing, Funding acquisition. **François Ganachaud:** Conceptualization, Validation, Formal analysis, Writing – review & editing, Supervision, Project administration, Funding acquisition.

Acknowledgement

The authors acknowledge Loïc DUMAZERT, Gwenn LE SAOULT and Antoine ISHAK, from IMT – Mines Alès for their support on cone calorimeter and XRD analyses and the preparation of black ceramic powder. The authors also acknowledge Carol GROSSIORD from Science et Surface for her support on XPS analyses. Fernande DA CRUZ-BOISSON is acknowledged for her help interpreting NMR data, and Pierre ALCOUFFE for assistance on MEB analyses. RH was supported by a grant from ANR (POLCADE ANR-17-CE07–0017).

Supplementary materials

Supplementary material associated with this article can be found, in the online version, at doi:10.1016/j.polymdegradstab.2022.109947.

References

[1] R.G. Jones, W. Ando, J. Chojnowski, Silicon-containing polymers, Springer, Netherlands, Dordrecht, 2000, doi:10.1007/978-94-011-3939-7.
[2] T. Köhler, A. Gutacker, E. Mejiá, Industrial synthesis of reactive silicones: reaction mechanisms and processes, Org. Chem. Front. 7 (2020) 4108–4120, doi:10.1039/d0qo01075h.
[3] B. Rupasinghe, J.C. Furgal, Full circle recycling of polysiloxanes via room-temperature fluoride-catalyzed depolymerization to repolymerizable cyclics, ACS Appl. Polym. Mater. 3 (2021) 1828–1839, doi:10.1021/acsapm.0c01406.
[4] R.R. Buch, D.N. Ingebrigtson, Rearrangement of poly (dimethylsiloxane) fluids on soil, Environ. Sci. Technol. 13 (1979) 676–679, doi:10.1021/es60154a002.
[5] D. Graiver, K.W. Farminer, R. Narayan, A Review of the fate and effects of silicones in the environment, J. Polym. Environ. 11 (2003) 129–136, doi:10.1023/A:1026056129717.
[6] S. Varaprath, R.G. Lehmann, Speciation and quantitation of degradation products of silicones (silane/siloxane diols) by gas chromatography-mass spectrometry and stability of dimethylsilanediol, J. Environ. Polym. Degrad. 5 (1997) 17–31, doi:10.1007/BF02763565.
[7] J.C. Furgal, C.U. Lenora, Green routes to silicon-based materials and their environmental implications, Phys. Sci. Rev. 5 (2020) 1–22, doi:10.1515/psr-2019-0024.
[8] A. Ghosh, R.S. Rajeev, A.K. Bhattacharya, A.K. Bhowmick, S.K. De, Recycling of silicone rubber waste: effect of ground silicone rubber vulcanizate powder on the properties of silicone rubber, Polym. Eng. Sci. 43 (2003) 279–296, doi:10.1002/pen.10024.
[9] S. Enthaler, Zinc-catalyzed depolymerization of end-of-life polysiloxanes, Angew. Chem. Int. Ed. 53 (2014) 2716–2721, doi:10.1002/anie.201309299.
[10] S. Enthaler, Iron-catalyzed depolymerization of polysiloxanes to produce dichlorodimethylsilane, diacetoxydimethylsilane, or dimethoxydimethylsilane, J. Appl. Polym. Sci. 132 (2015) 1–8, doi:10.1002/app.41287.
[11] M. Weidauer, B. Heyder, D. Woelki, M. Tschiersch, A. Köhler-Krützfeldt, S. Enthaler, Iron-catalyzed depolymerizations of silicones with hexanoic anhydride provide a potential recycling method for end-of-life polymers, Eur. J. Lipid Sci. Technol. 117 (2015) 778–785, doi:10.1002/ejlt.201400592.
[12] D.J. Krug, M.Z. Asuncion, R.M. Laine, Facile approach to recycling highly cross-linked thermoset silicone resins under ambient conditions, ACS Omega 4 (2019) 3782–3789, doi:10.1021/acsomega.8b02927.
[13] M. Okamoto, S. Suzuki, E. Suzuki, Polysiloxane depolymerization with dimethyl carbonate using alkali metal halide catalysts, Appl. Catal. A-Gen. 261 (2004) 239–245, doi:10.1016/j.apcata.2003.11.005.
[14] M.R. Alexander, F.S. Mair, R.G. Pritchard, J.E. Warren, Mild depolymerization of silicone grease using aluminum(III) chloride: high-yield synthesis and crystal structure of $[\{ClSiMe_2OAlCl_2\}_2]$, and its controlled hydrolysis on aluminum surfaces, Appl. Organomet. Chem. 17 (2003) 730–734, doi:10.1002/aoc.500.
[15] P. Döhlert, S. Enthaler, Depolymerization protocol for linear, branched, and crosslinked end-of-life silicones with boron trifluoride diethyl etherate as the depolymerization reagent, J. Appl. Polym. Sci. 132 (2015) 1–7, doi:10.1002/app.42814.
[16] H.S. Booth, M.L. Freedman, Cleavage of silicones by hydrogen fluoride, J. Am. Chem. Soc. 72 (1950) 2847–2850, doi:10.1021/ja01163a007.
[17] C.L. Chang, H.S.J. Lee, C.K. Chen, Nucleophilic cleavage of crosslinked polysiloxanes to cyclic siloxane monomers: mild catalysis by a designed polar solvent system, J. Polym. Res. 12 (2005) 433–438, doi:10.1007/s10965-004-1871-1.
[18] Z. Ren, S. Bin Mujib, G. Singh, High-temperature properties and applications of Si-based polymer-derived ceramics: a review, Materials (Basel) 14 (2021) 1–18, doi:10.3390/ma14030614.
[19] E. Delebecq, S. Hamdani-Devarennes, J. Raeke, J.M. Lopez Cuesta, F. Ganachaud, High residue contents indebted by platinum and silica synergistic action during the pyrolysis of silicone formulations, ACS Appl. Mater. Interfaces 3 (2011) 869–880, doi:10.1021/am101216y.
[20] T. Liu, X. Zeng, X. Lai, H. Li, Efficient organic-to-inorganic conversion of polysiloxane by novel platinum-thiol catalytic system, Polym. Degrad. Stab. 176 (2020) 109161, doi:10.1016/j.polymdegradstab.2020.109161.
[21] T. Liu, X. Zeng, X. Lai, H. Li, Y. Wang, Remarkable improvement of organic-to-inorganic conversion of silicone rubber at elevated temperature through platinum-nitrogen catalytic system, Polym. Degrad. Stab. 171 (2020) 109026, doi:10.1016/j.polymdegradstab.2019.109026.
[22] W. Chen, X. Zeng, X. Lai, H. Li, W. Fang, T. Liu, Synergistic effect and mechanism of platinum catalyst and nitrogen-containing silane on the thermal stability of silicone rubber, Thermochim. Acta. 632 (2016) 1–9, doi:10.1016/j.tca.2016.03.008.
[23] L. Shen, W. Qiu, B. Liu, Q. Guo, Stable superhydrophobic surface based on silicone combustion product, RSC Adv. 4 (2014) 56259–56262, doi:10.1039/c4ra10838h.
[24] A. Stricher, L. Picard, B. Gabrielle, E. Delebecq, F. Ganachaud, Influence of the microstructure of gums on the mechanical properties of silicone high consistency rubbers, Polym. Int. 65 (2016) 713–720, doi:10.1002/pi.5131.
[25] S. Hamdani-Devarennes, A. Pommier, C. Longuet, J.M. Lopez-Cuesta, F. Ganachaud, Calcium and aluminium-based fillers as flame-retardant additives in silicone matrices II. Analyses on composite residues from an industrial-based pyrolysis test, Polym. Degrad. Stab. 96 (2011) 1562–1572, doi:10.1016/j.polymdegradstab.2011.05.019.
[26] E. Delebecq, F. Ganachaud, Looking over liquid silicone rubbers: (1) network topology vs chemical formulations, ACS Appl. Mater. Interfaces 4 (2012) 3340–3352, doi:10.1021/am300502r.
[27] P.J. Flory, J. Rehner, Statistical mechanics of cross-linked polymer networks I. Rubberlike elasticity, J. Chem. Phys. 11 (1943) 512–520, doi:10.1063/1.1723791.
[28] P. Vondráček, A. Pouchelon, Ammonia-induced tensile set and swelling in silica-filled silicone rubber, Rubber Chem. Technol. 63 (1990) 202–214, doi:10.5254/1.3538251.
[29] P. Vondráček, M. Schätz, NH_3-modified swelling of silica-filled silicone rubber, J. Appl. Polym. Sci. 23 (1979) 2681–2694, doi:10.1002/app.1979.070230913.
[30] C. Huggett, Estimation of rate of heat release by means of oxygen consumption measurements, Fire Mater. 4 (1980) 61–65, doi:10.1002/fam.810040202.
[31] M. de Almeida Silva, É.S. Romagnoli, R. de Carvalho Pereira, C.R.T. Tarley, M.G. Segatelli, Structure and porosity of silicon oxycarbide/carbon black composites, Mater. Chem. Phys. (2020) 254, doi:10.1016/j.matchemphys.2020.123503.
[32] T. Gumula, C. Paluszkiewicz, M. Blazewicz, Structural characterization of polysiloxane-derived phases produced during heat treatment, J. Mol. Struct. 704 (2004) 259–262, doi:10.1016/j.molstruc.2003.12.064.
[33] H.-J. Kleebe, G. Gregori, F. Babonneau, Y.D. Blum, D.B. MacQueen, S. Masse, Evolution of C-rich SiOC ceramics, Int. J. Mater. Res. 97 (2006) 699–709, doi:10.3139/146.101292.
[34] H.J. Kleebe, Y.D. Blum, SiOC ceramic with high excess free carbon, J. Eur. Ceram. Soc. 28 (2008) 1037–1042, doi:10.1016/j.jeurceramsoc.2007.09.024.
[35] K.S. Bagdasar'Ian, Z.A. Sinitsina, Polymerization inhibition by aromatic compounds, J. Polym. Sci. 52 (1961) 31–38, doi:10.1002/pol.1961.1205215704.
[36] S.C. Shit, P. Shah, A review on silicone rubber, Natl. Acad. Sci. Lett. 36 (2013) 355–365, doi:10.1007/s40009-013-0150-2.
[37] F.Y. Hshieh, Shielding effects of silica-ash layer on the combustion of silicones and their possible applications on the fire retardancy of organic polymers, Fire Mater. 22 (1998) 69–76 https://doi.org/10.1002/(sici)1099-1018(199803/04)22:2⟨69::aid-fam640⟩3.3.co;2-l.